

# Strontium-Delivering Glasses with Enhanced Bioactivity: A New Biomaterial for Antiosteoporotic Applications?

Jonathan Lao,<sup>†</sup> Edouard Jallot,<sup>†</sup> and Jean-Marie Nedelec<sup>\*,‡</sup>

*Laboratoire de Physique Corpusculaire, CNRS/IN2P3 UMR 6533, Université Blaise Pascal, 24 avenue des Landais, 63177 Aubière Cedex, France, and Laboratoire des Matériaux Inorganiques, CNRS UMR 6002, Université Blaise Pascal & Ecole Nationale Supérieure de Chimie de Clermont-Fd, 24 avenue des Landais, 63177 Aubière Cedex, France*

Received March 3, 2008. Revised Manuscript Received May 9, 2008

Bioactive glasses exhibit great performances for bone tissue regeneration. In biological conditions, they spontaneously bond to bone tissues while actively stimulating bone growth. Crucial parameters for the material's bioactivity are the kinetics of formation of the interfacial calcium phosphate layer at the glass surface, as well as the release of critical concentrations of ionic dissolution products capable of stimulating cellular responses. In this paper we report the remarkable bioactivity properties of strontium-delivering sol–gel-derived glasses in the  $\text{SiO}_2$ – $\text{CaO}$ – $\text{SrO}$  system. The glasses were tested in vitro and the interface between the glass and the biological medium was chemically mapped using highly sensitive nuclear microprobes. We prove the ability of our materials to form a phosphocalcic layer at their periphery with increased kinetics of reaction. Our key result is the demonstration that Sr-doped glasses can deliver controlled doses of strontium toward the biological medium. That is the determinant for bone tissue regeneration, as far as strontium is known to positively act on bone remodeling. Sr-delivering glasses could further represent an alternative to the constraining oral administration of strontium in treatment of osteoporosis.

## Introduction

Biomaterials are intended to interface with biological systems to treat, augment, or replace any tissue, organ, or function of the body. Among ceramic biomaterials, bioactive glasses exhibit great performances for bone tissue regeneration. In biological conditions, they spontaneously bond to bone tissues while actively stimulating bone growth. The bone-bonding ability relies on the formation of an interfacial apatite-like layer at the glass surface, the composition being close to the mineral phase of bone.<sup>1</sup> In addition, the osteoinduction properties of bioactive glasses are due to the release of critical concentrations of ionic dissolution products that cause rapid expression of genes regulating osteogenesis and the production of growth factors. Rapid new bone formation is encouraged through the stimulation of both intracellular and extracellular responses.<sup>2</sup> Over the past few years great efforts have been made in optimizing the textural properties of bioactive glasses.<sup>3</sup> However, both the texture and composition of a glass are interdependent parameters

that are closely related to the material's bioactive properties; hence, studying the influence of the glass matrix composition should not be neglected. A major advantage with glasses is that any property of the material can be varied continuously by finely tuning its chemical composition: in this sense few studies deal with the effect of doping a glass matrix onto its bioactive properties. The main reason is that few characterization methods provide sufficient sensitivity to highlighting the subtle but determinant changes in the bioactivity mechanism. In this paper we report the remarkable bioactive properties of strontium-delivering sol–gel-derived glasses in the  $\text{SiO}_2$ – $\text{CaO}$ – $\text{SrO}$  ternary system.

Strontium is a naturally occurring trace element in the human body but it has attracted less attention than other important metals such as Ca or Mg. With the development of the drug strontium ranelate (Protelos, Servier Laboratories, France), which has been found to reduce the incidence of fractures in osteoporotic patients, a growing awareness of the biological role of Sr has arisen.<sup>4</sup> Osteoporosis is characterized by low bone mass and thus increased susceptibility to fracture. Sr has been demonstrated to promote bone formation and osteoblasts replication while inhibiting bone resorption by osteoclasts.<sup>5</sup> The singular properties of the

\* Corresponding author. Tel.: +33 (0)4 73 40 71 95. Fax: +33 (0)4 73 40 53 28. E-mail: j-marie.nedelec@univ-bpclermont.fr.

<sup>†</sup> CNRS/IN2P3 UMR 6533, Université Blaise Pascal.

<sup>‡</sup> CNRS UMR 6002, Université Blaise Pascal & Ecole Nationale Supérieure de Chimie de Clermont-Fd.

- (a) Hench, L. L. *J. Am. Ceram. Soc.* **1998**, *81*, 511. (b) Yuan, H.; De Brujin, J. D.; Zhang, X.; Van Blitterswijk, C. A.; De Groot, K. *J. Biomed. Mater. Res.* **2001**, *58*, 270. (c) Livingston, T.; Ducheyne, P.; Garino, J. *J. Biomed. Mater. Res.* **2002**, *62*, 1. (d) Yli-Urpo, H.; Lassila, L. V. J.; Naerhi, T. O.; Vallittu, P. K. *Dent. Mater.* **2005**, *21*, 201.
- (2) (a) Hench, L. L.; Polak, J. M. *Science* **2002**, *295*, 1014. (b) Radin, S.; Reilly, G.; Bhargave, G.; Leboy, P. S.; Ducheyne, P. *J. Biomed. Mater. Res. A* **2005**, *73*, 21.

- (3) (a) Jones, J. R.; Ehrenfried, L. M.; Hench, L. L. *Biomaterials* **2006**, *27*, 964. (b) Yan, H.; Zhang, K.; Blanford, C. F.; Francis, L. F.; Stein, A. *Chem. Mater.* **2001**, *13*, 1374. (c) Padilla, S.; Sánchez-Salcedo, S.; Vallet-Regi, M. *J. Biomed. Mater. Res.* **2007**, *81*, 224.
- (4) (a) Ortolani, S.; Vai, S. *Bone* **2006**, *38*, S19. (b) Pors-Nielsen, S. *Bone* **2004**, *35*, 583.
- (5) Meunier, P. J.; Roux, C.; Seeman, E.; Ortolani, S.; Badurski, J. E.; Spector, T. D.; Cannata, J.; Balogh, A.; Lemmel, E. M.; Pors-Nielsen, S. *N. Engl. J. Med.* **2004**, *350*, 459.

strontium ranelate molecule, composed of an organic moiety which binds two strontium atoms, are based on the delivery of  $\text{Sr}^{2+}$ ; indeed the specific effects of strontium ranelate were not reproduced by calcium ranelate, suggesting a distinct effect of the two cations.<sup>6</sup> The development of biomaterials for applications in bone tissue regeneration calls for engineering structure that will provide the support for the body to manage reconstruction; in this sense designing Sr-delivering materials had drawn our full attention. Recently, Xue *et al.* also demonstrated the enhanced adhesion and differentiation of osteoprecursors cells in contact with Sr-substituted hydroxyapatite.<sup>7</sup> We synthesized mesoporous Sr-doped glasses in the  $\text{SiO}_2$ – $\text{CaO}$ – $\text{SrO}$  system using the sol–gel process. The bioactive properties of the materials were tested *in vitro* by immersion in a biological medium. Their ability to deliver Sr in physiological concentrations both at the material surface and within the medium via a controlled leaching of ions was evaluated; for these purposes nuclear microprobes were used to chemically map the glass/biological medium interface, while the evolution of elemental concentrations in the biological medium was followed through ICP-AES measurements.

## Experimental Section

**Preparation of the Bioactive Glass Samples.** The sol–gel method was used to synthesize mesoporous Sr-doped bioactive glasses. The sol–gel process provides materials with an excellent chemical homogeneity: this is a very crucial point as far as doping is concerned.<sup>8</sup> Three materials were prepared: one undoped glass in the binary  $\text{SiO}_2$ – $\text{CaO}$  system, named B75, and two Sr-doped glasses in the  $\text{SiO}_2$ – $\text{CaO}$ – $\text{SrO}$  system, named B75–Sr1 and B75–Sr5. The glasses labeled B75–SrX are of chemical composition  $\text{SiO}_2$ (75 wt %)– $\text{CaO}$ (25–X wt %)– $\text{SrO}$ (X wt %). Tetraethylorthosilicate ( $\text{Si}(\text{OC}_2\text{H}_5)_4$ ), calcium nitrate  $\text{Ca}(\text{NO}_3)_2 \cdot 4\text{H}_2\text{O}$ , and strontium nitrate  $\text{Sr}(\text{NO}_3)_2$  (Sigma-Aldrich) were mixed in ethanol in the presence of water and HCl under ambient pressure. The prepared sols were then transferred to an oven at 60 °C for gelification and aging. Four hours later, the obtained gels were dried at 125 °C for 24 h, then ground to a powder, and stabilized at 700 °C to achieve nitrate elimination and further densification. The corresponding heating schedule was as follows: a furnace was programmed to heat up from room temperature to 700 °C with a 10 °C/min rate, then the samples were heated at 700 °C for 24 h, and finally they were allowed to cool down to room temperature. The dry powders were compacted into discs of 13 mm diameter and 2 mm height without any additive.

**Materials Characterization.** The chemical compositions of the bioactive glass powders were determined by inductively coupled plasma-atomic emission spectroscopy (ICP-AES). The experimental glass compositions are given in Table 1. They are close to the expected nominal values. One can note that the total amount in oxide sums up to about 97%; indeed, because of their high alkaline-earth content, the glasses are highly reactive toward water and thus can easily become hydrated in contact with the air. Furthermore, ambient carbon dioxide can penetrate into the highly porous samples, condensing at the materials surface to form calcium carbonate.

(6) Marie, P. J. *Curr. Opin. Pharm.* **2005**, 5, 633.

(7) Xue, W.; Moore, J. J.; Hosick, H. L.; Bose, S.; Bandyopadhyay, A.; Lu, W. W.; Cheung, K. M. C.; Luk, K. D. K. *J. Biomed. Mater. Res. A* **2006**, 79A, 804.

(8) (a) Hench, L. L.; West, J. K. *Chem. Rev.* **1990**, 90, 33. (b) Li, P.; De Groot, K. J. *Sol–Gel Sci. Technol.* **1994**, 2, 797.

**Table 1. Composition of the Sol–Gel-Derived B75, B75–Sr1, and B75–Sr5 Glasses (wt %) as Determined by ICP-AES**

	B75	B75–Sr5	B75–Sr5
$\text{SiO}_2$	$72.20 \pm 0.37$	$74.22 \pm 0.52$	$74.08 \pm 0.51$
$\text{CaO}$	$24.50 \pm 0.17$	$23.60 \pm 0.17$	$19.03 \pm 0.13$
$\text{SrO}$		$0.83 \pm 0.08$	$3.83 \pm 0.04$

**Table 2. Textural Properties of the Gel–Glass Powders<sup>a</sup>**

	B75	B75–Sr1	B75–Sr5
BET surface area ( $\text{m}^2/\text{g}$ )	30	24	28
BJH average pore diameter (nm)	8.4	11.8	9.3
BJH modal pore diameter (nm)	4.6	6.1	4.7
total pore volume ( $\text{cm}^3/\text{g}$ )	0.062	0.069	0.066

<sup>a</sup> The surface area ( $S$ ) was determined from the linear portion of the BET plot, the total pore volume ( $V$ ) was estimated from the amount of  $\text{N}_2$  adsorbed at  $P/P_0 = 0.995$ , the pore size distribution and the modal pore diameter were calculated by applying the BJH method to the  $\text{N}_2$  desorption branches, and the average pore diameter was calculated as  $r = 2V/S$ .

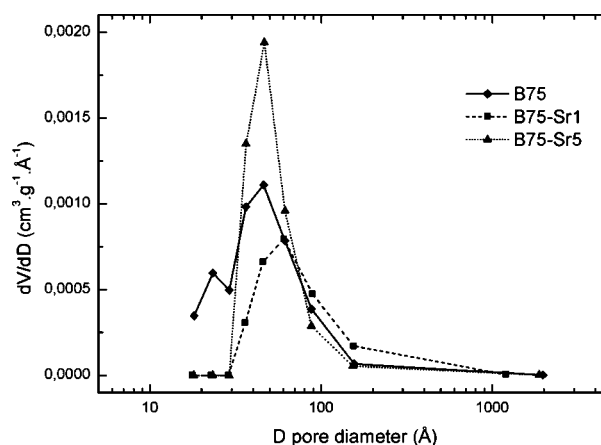


**Figure 1.** Pore size distributions for all the glasses.

The textural characterization of the samples was performed by nitrogen gas sorption analyses. The samples were vacuum outgassed at 120 °C for 12 h to remove physically adsorbed molecules such as moisture from the pores. The adsorption/desorption isotherms were recorded on a Quantachrom Autosorb-1 apparatus. The instrument determined isotherms volumetrically by a discontinuous static method at 77 K. The surface areas were obtained by applying the BET method to the  $\text{N}_2$  isotherm. The pore size distribution was determined by the BJH method on the desorption branch. Total pore volume was measured at a relative pressure  $P/P_0 = 0.995$ .

Table 2 shows the results for the BET surface area, for the average and modal pore diameters, and for the total pore volume. The surface area and the total pore volume do not significantly change with addition of strontium. Very wide pore size distributions were observed for all the glasses: the pores ranged from 3 to 80 nm in diameter, as evidenced by Figure 1. Calcium and strontium, as network modifiers, cause discontinuity in the glassy network, resulting in the formation of nonbridging oxygens.

**In Vitro Studies.** The glass discs were immersed at 37 °C for 1 h, 6 h, 1 day, 2 days, 5 days, and 10 days in 45 mL of a standard Dulbecco's Modified Eagle Medium (DMEM, Biochrom AG, Germany): DMEM contains inorganic salts, glucose, amino acids, and vitamins and is widely used for cell culture. The inorganic salts concentrations in DMEM are almost equal to human plasma (cf. Supporting Information). Because proteins are present in DMEM, lower rates for the materials dissolution and a subsequent delay in surface layer formation are to be expected when compared to soaking in Simulated Body Fluids (SBF is strictly an electrolyte solution); indeed, proteins from DMEM are charged species that

can be attracted by the negative glass surface and coat it with a film.<sup>9</sup> However, DMEM grants better testing conditions to simulate a biological environment; moreover, it is commonly used as an osteoblast culture media. Thus, we decided to use it in the present study in view of confronting further biological results. After interaction, part of the DMEM was analyzed by ICP-AES while the glass discs were removed from the solution and air-dried. SEM analyses were conducted over the glass discs after different interaction periods to follow up the surface changes. Results are available in the Supporting Information and provide us with the same observations that are available in the abundant literature. After soaking, the discs' surface is quickly coated with small calcium phosphate precipitates. Initially limited to some scattered sites, the newly formed surface layer quickly extends over the whole material. The CaP precipitates progressively crystallize by incorporation of anions from DMEM. Before characterization with nuclear microprobes, the glass discs were embedded in resin (AGAR, Essex, England) and then cut into thin sections of 30  $\mu\text{m}$  nominal thickness using a Leica RM 2145 microtome. Finally, the sections were placed on a Mylar film with a hole of 3 mm in the center. Measurements with nuclear microprobes were performed on the area of the section placed over the hole.

**PIXE-RBS Analyses.** The glass/biological medium interface was studied using the highly sensitive PIXE-RBS nuclear microprobes (PIXE, particle-induced X-ray emission; RBS, Rutherford back-scattering spectrometry): these techniques allowed chemical mapping of the glass/biological medium interface through the detection of fluorescence X-rays. The key advantage of the method is the possibility to accurately quantify the elemental concentrations (up to the  $10^{-6}\text{g/g}$  level) in user-defined regions of interest. PIXE and RBS methods are used simultaneously. The PIXE method permits the identification and the quantification of major and trace elements at the biomaterial/biological fluids interface. RBS is used to determine the electric charge received by the samples during irradiation. This parameter is absolutely necessary for PIXE spectra quantification.

Analyses of the biomaterial/biological fluids interface were carried out using nuclear microprobes at the CENBG (Centre d'Études Nucléaires de Bordeaux-Gradignan, France). For PIXE-RBS analyses, we chose proton scanning microbeam of 2.9 MeV energy and 500 pA in intensity. The beam size was 2  $\mu\text{m}$ . Such settings resulted in higher ionization cross sections and an increased sensitivity for the micro-PIXE analysis. Furthermore, weak intensities and the choice of protons as the ion beam allowed the target degradation to be minimized during irradiation. However, the intensities were sufficient to permit measurement duration under 1 h.

An 80 mm<sup>2</sup> Si(Li) detector was used for X-ray detection, orientated at 135° with respect to the incident beam axis and equipped with a beryllium window 12  $\mu\text{m}$  thick. An Al filter with a tiny 500  $\mu\text{m}$  hole drilled at its center ("funny filter") was systematically placed in front of the Si(Li) detector. The funny filter allows the detection of heavy trace elements ( $Z \geq 25$ ) whereas it avoids the saturation of the detector by major light ( $Z \leq 20$ ) elements X-rays since the latter are only detected through the small aperture. PIXE spectra were treated with the software package GUPIX. In relation to RBS, a silicon particle detector was placed at 135° from the incident beam axis and allowed the determination of the number of protons that interacted with the sample. Data were treated with the SIMNRA code. This methodology finally allowed quantification of major and trace elements concentrations.

(9) (a) Sepulveda, P.; Jones, J. R.; Hench, L. L. *J. Biomed. Mater. Res.* **2002**, *61*, 301. (b) Lobel, K. D.; Hench, L. L. *J. Sol-Gel Sci. Technol.* **1996**, *7*, 69.

## Results and Discussion

Interactions between glasses and a biological medium lead to physicochemical reactions resulting in intense ionic exchanges. Briefly, two mechanisms occur: hydrolysis from biological fluids causes dissolution of the glass silicate network, while a surface layer quickly forms at the material periphery. The in vitro bioactivity of B75 has already been discussed in our previous works<sup>10</sup> and we will use it as a basis for comparison with Sr-doped glasses. Figure 2 shows the elemental distributions at the periphery (0–175  $\mu\text{m}$  deep from the glass surface) of a B75-Sr5 disk after 10 days of interaction with DMEM. Similar results were obtained for the B75-Sr1 glass (cf. Supporting Information). A Ca–P-rich layer has formed at the surface of the disk and extends over 15  $\mu\text{m}$ . The layer results from the incorporation of P, taken from the biological medium, and Ca, which comes from both the glass matrix and the biological medium. Substantial amounts of Si remain at the glass surface; indeed, a high surface area silica hydrogel is known to form during the bioactivity process, resulting from the polycondensation reactions of  $-\text{SiOH}$  surface silanols. This porous hydrated silica layer grants low interfacial energies and thus provides a large number of specific favorable sites for the nucleation and growth of calcium phosphates.<sup>11</sup> One major observation is that traces of Sr, which is initially present in the glass matrix, and traces of Mg, coming from the biological medium, are incorporated at the material surface, within the newly formed phosphocalcic layer. This is a very engaging result for further bone tissue engineering developments; one can easily imagine the benefits of implanting a bioactive material providing both Sr, which positively acts on bone remodeling, and Mg, which possesses anti-inflammatory and bactericidal properties.<sup>12</sup> Calculation of elemental concentrations within the peripheral layer was performed; the results are displayed in Table 3.

Beyond the Ca–P peripheral layer, in the inner part of the disk, we observe a region where the silicate network has been almost completely broken down because of its hydrolysis by biological fluids. Great quantities of Ca are detected in this area, as mobile  $\text{Ca}^{2+}$  ions diffuse from the core of the material to its periphery. For the same reason important  $\text{Sr}^{2+}$  concentration is observed in this region, while  $\text{Mg}^{2+}$  from biological fluids easily migrates through the glass network, reaching the inner parts of the material. The core of the material (data not shown) consists of the silicate network with composition close to that of the primary glass.

To identify the nature of the phases precipitating at the surface of glass particles, we recorded X-Ray diffraction (XRD) patterns before and after interaction. No difference or any signal corresponding to a crystalline phase was

(10) (a) Lao, J.; Nedelec, J. M.; Moretto, P.; Jallot, E. *Nucl. Instrum. Methods B* **2006**, *245*, 511. (b) Lao, J.; Nedelec, J. M.; Jallot, E. *J. Phys. Chem. C* **2008**, *112*, 9418.  
 (11) Ohtsuki, C.; Kokubo, T.; Yamamuro, T. *J. Non-Cryst. Solids* **1992**, *143*, 84.  
 (12) (a) Weglicki, W. B.; Phillips, T. M.; Freedman, A. M.; Cassidy, M. M.; Dickens, B. F. *Mol. Cell. Biochem.* **1992**, *110*, 169. (b) Rijkers, G. T.; Henriquez, N.; Griffioen, A. W. *Magn. Res.* **1993**, *6*, 205. (c) Almoznino-Sarafian, D.; Berman, S.; Mor, A.; Shteinshnaider, M.; Gorelik, O.; Tzur, I.; Alon, I.; Modai, D.; Cohen, N. *Eur. J. Nutr.* **2007**, *46*, 230.

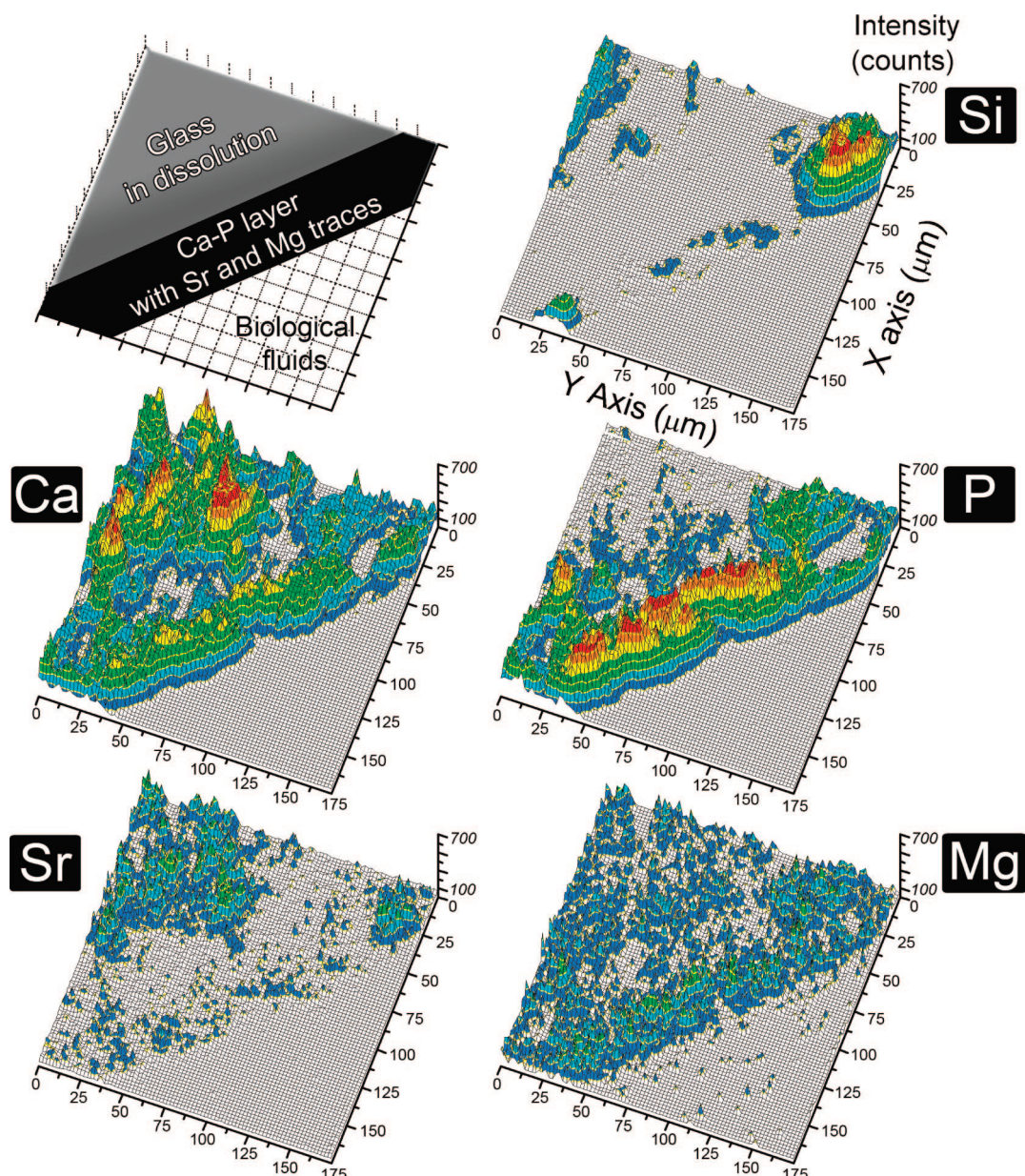


**Figure 2.** Chemical mapping at the periphery of a B75-Sr5 glass disk after 10 days of interaction with biological fluids ( $175 \times 175 \mu\text{m}^2$ ).

**Table 3. Elemental Concentrations at the Periphery of Sr-Doped Glasses after 10 Days of Interaction (wt %)**

	Ca	P	Si	Sr	Mg
B75-Sr1	32.4	12.4	5.7	0.4	1.9
B75-Sr5	29.9	13.1	9.4	0.8	1.2

observed. The very thin layer that is formed makes the characterization by XRD difficult. Furthermore, in these early stages of biomimetic mineralization, the solid is poorly crystallized so that no long-range order is observed. Local diffraction techniques (micro diffraction setup at synchrotron beamlines or electronic diffraction<sup>13</sup>) could help in such characterization but fall beyond the scope of this first report.

To further investigate the glasses bioactivity, we calculated the Ca/P atomic ratios at the materials surface by creating thin regions of measurement 1  $\mu\text{m}$  wide at the glass/

biological fluids interface. In fact, the formation of insoluble apatite crystals at the glasses surface involves the formation of metastable phosphocalcic phases. Hydroxyapatite is at physiological pH thermodynamically the most stable and the least soluble of all calcium phosphates, but the formation of apatite-like crystals at the glasses surface experience a number of kinetics processes, which take place at different rates and involve more than one phosphocalcic phase. Therefore, studying the Ca/P atomic ratios at the glasses surface gives essential indication of the evolution of the phosphocalcic layer. Results have been plotted as a function of interaction time in Figure 3. They shall be compared to the 1.67 Ca/P value of stoichiometric hydroxyapatite, although the apatite-like layer present at the glasses surface actually consists of a mixture of poorly crystallized and substituted apatite nanocrystals. After 10 days of interaction, the Ca/P atomic ratio is equal to 1.8 for B75-Sr1 and B75-Sr5, very close to the nominal value of HA, whereas it is

(13) Vallet-Regí, M.; Salinas, A. J.; Ramírez-Castellanos, J. R.; González-Calbet, J. M. *Chem. Mater.* 2005, 17, 1874.

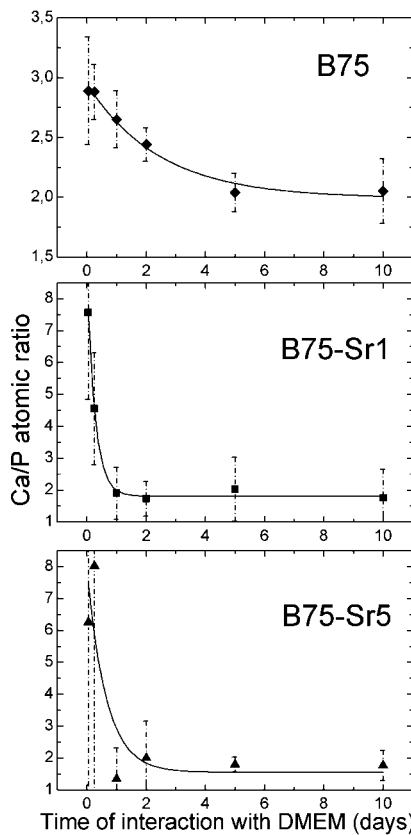


**Figure 3.** Evolution of the Ca/P atomic ratio at the glasses surface as a function of interaction time.

equal to 2.1 for B75. Moreover, Figure 3 shows that the exponential-like decrease of the Ca/P atomic ratio is faster for Sr-doped glasses. There lies another surprising property of Sr-doped glasses: the bioactivity process more quickly leads to a stable phosphocalcic layer.

Finally, the ICP-AES analyses of DMEM confirm the previous observations. The biological medium becomes poorer in calcium, phosphate, and magnesium ions with increasing time of interaction. These ions are used to feed the growth of the phosphocalcic layer at the glasses surface. Ca and Mg concentrations in the medium decrease more quickly for Sr-doped glasses when compared to those for the undoped B75 sample, as a result of their greater kinetics of HA precipitation. For both B75-Sr1 and B75-Sr5, after 10 days of interaction, 62 ppm Ca and 15 ppm Mg are detected in DMEM; for the undoped B75, at the same interaction time, 94 ppm Ca and 18 ppm Mg remain. Furthermore, Sr is partially released from the glasses surface into the initially Sr-free biological medium (Figure 4). After 10 days of interaction, the amount of Sr released is equal to 1 ppm for B75-Sr1 and 5 ppm for B75-Sr5. Such Sr quantities are interesting for osteoporosis therapy: indeed, they are in the same order of magnitude as those measured *in vivo* in plasmas of animals treated with Sr-based drugs (i.e., strontium ranelate) which were found to have obvious

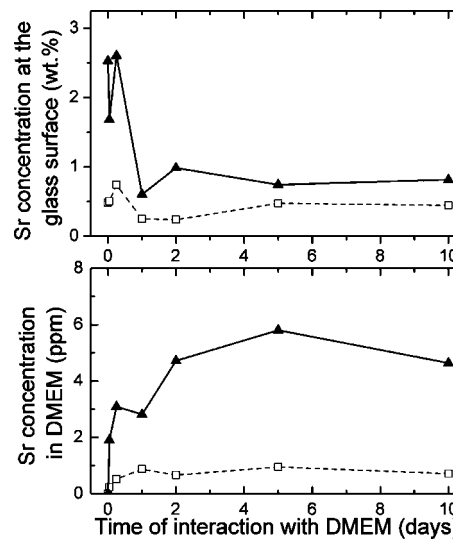


**Figure 4.** Sr concentration (□, B75-Sr1; ▲, B75-Sr5) at the glasses surface and in DMEM as a function of interaction time.

antiosteoporotic effects.<sup>14</sup> B75-Sr5 delivers 5 times more Sr than B75-Sr1, perfectly agreeing with the initial Sr content in the glass matrixes. This is an essential result in view of delivering controlled doses of Sr.

## Conclusion

The enhanced bioactivity of Sr-doped bioactive glasses has been demonstrated *in vitro*. Sr-doped glasses are able to induce the formation of a bonelike apatite layer at their periphery with increased kinetics of reaction. The ability of our materials to (i) provide interesting Sr quantities at the interface with the biological medium and (ii) to deliver critical concentrations of Sr under physiological conditions are key parameters for bone tissue regeneration and antiosteoporotic applications. These remarkable properties stimulate extensive investigations for designing Sr-delivering bioactive glass scaffolds for tissue engineering.

**Acknowledgment.** This work was supported by ANR in the National Program of Nanosciences and Nanotechnologies PNANO2005 (project “BIOVERRES” no. ANR-05-NANO-040). Philippe Moretto and the AIFIRA team are gratefully acknowledged for their help with PIXE-RBS measurements at the CENBG.

**Supporting Information Available:** DMEM ionic concentrations, SEM images of the glass surface before and after interaction in DMEM, and chemical mapping at the periphery of the B75-Sr1 disk after 10 days of interaction (PDF). This material is available free of charge via the Internet at <http://pubs.acs.org>.

CM800993S

(14) Dahl, S. G.; Allain, P.; Marie, P. J.; Mauras, Y.; Boivin, G.; Ammann, P.; Tsouderos, Y.; Delmas, P. D.; Christiansen, C. *Bone* **2001**, 28, 446.